Ceylon Journal of Science: Physical Sciences, 4(1), 23-32 (1997)

CONSTRUCTION OF A keV PULSED ION SOURCE AND THE MEASUREMENT OF DAMAGE CROSS-SECTIONS FOR keV ION INDUCED SPUTTERING FROM SOLID TARGETS

D. D. N. BARLO DAYA, T. R. ARIYARATNE
Department of Physics, University of Colombo, Colombo - 3, Sri Lanka.
P. HÅKANSSON AND B. U. R. SUNDQVIST
Division of Ion Physics, Department of Radiation Sciences, Uppsala University, Box 535, S-751 21 Uppsala, Sweden.
W. ENS
Department of Physics, University of Manitoba, Winnipeg, Manitoba, R3T, 2N2, Canada.

ABSTRACT

A pulsed, low energy (keV), primary ion source has been constructed and coupled to an existing plasma desorption time-of-flight mass spectrometer. Pulses of Cs^+ primary ions (1 - 30 keV) of about 2 ns duration have been obtained from the source and used to measure the damage cross sections for keV ion induced sputtering from amino acid valine (MW=117 u) and Luteinizing Hormone Releasing Hormone (LHRH) (MW=1182 u). Sputtered targets were examined with the time-of-flight mass spectrometer. Irradiation for damage measurements was carried out by operating the ion source in the DC mode. The variation of the secondary molecular ion yield as a function of the intensity of the primary ion flux has been measured and used to evaluate damage cross sections and the values were found to be in the order of 10^{-14} cm^2. These values are one order of magnitude lower than the previously published corresponding values for the high energy (MeV) ion irradiated valine.

1. INTRODUCTION

With the introduction of the technique, now known as plasma desorption mass spectrometry (PDMS) by Macfarlane and co-workers[1] in 1974, there has been a renewed interest in the determination of the molecular weight of heavy biomolecules using this technique. In such a mass spectrometer, a ^{252}Cf radioactive source serves as a primary ion source and, one of the two simultaneous fragments produced by the fission of ^{252}Cf is used to start the time-of-flight (TOF) measurement and the other is used to desorb molecular ions from the sample surface.

In the present study, in addition to the ^{252}Cf source, a pulsed low energy ion source (1-30 keV) of Cs^+ ions has been constructed and coupled to an existing PDMS-TOF mass spectrometer. This combination provided the opportunity of mass analysing a given sample using primary ions in both MeV or keV energy regions, and to study irradiation effects of MeV and keV ions on surfaces. Here the experimental set-up has been used to measure so called damage cross sections for some organics bombarded by keV ions.

1.1 Damage cross section

When a target (containing organic molecules) is irradiated with energetic ions, desorption of some material containing molecular ions, as well as damage to the surface close to the regions where primary ions impinge will occur. As a consequence of this damage, the yield of molecular ions desorbed is expected to decrease with the radiation dose. For such situations, a quantity called damage cross section, σ, can be defined which depicts the damaged area per single primary ion. The measured molecular ion yield from an irradiated surface can be related[2] to σ by

$$Y = Y_0[A-S(n,\sigma)]/A \qquad (1)$$

where Y_0 is the yield of the unfragmented molecular ions before irradiation; Y is the corresponding yield after the sample has been irradiated with n number of primary ions; A is the irradiated surface area of the sample and S is the total damaged area due to the incident ions. As Y_0, Y and A can be measured experimentally, σ can be found if an expression for $S_{(n,\sigma)}$ in terms of known quantities is obtained. σ, will take care of all effects that reduce the yield of molecular ions due to irradiation, and they include both prompt effects as well as late chemical effects. Assume that each particle in a beam of particles that strikes a sample surface area A, damages an area of σ. If the first particle damages an area σ with a probability of 1, then the second particle will damage the same area (σ) with a lower probability of $1-(\sigma/A)$. Then it follows that

$$S_n = S_{n-1} + [1-(S_{n-1}/A)]\sigma$$

where S_n is the total damaged area after the n^{th} particle has impinged on the sample surface. Then

$$dS/dn = \sigma - (\sigma/A)S$$

and

$$S = A[1-\exp(-\sigma n/A)]$$

By substituting S in equation (1), an expression for the yield Y is obtained that includes the damage cross section σ :

$$Y = Y_0 \exp(-\sigma n/A) \qquad (2)$$

Therefore, the gradient of a plot of lnY vs n/A can be used to evaluate the damage cross section σ.

2. THE CONSTRUCTION OF THE PULSED ION SOURCE

2.1 The keV ion source

The pulsed ion gun similar to that of Chait & Standing[3] was constructed and is shown schematically in figure 1. The source of ions is a small bead (1 mm diameter) of cesium aluminosilicate[4,5] melted onto the end of a tungsten hairpin filament. The bead is prepared by dipping the end of the tungsten hairpin into a mixture of cesium aluminosilicate in amyl acetate and heating it in a flame for a few seconds. This procedure is repeated several times until the bead becomes about 1 mm in diameter. Other alkali metal ions such as Li^+, Na^+or K^+ can also

be incorporated in place of Cs^+ ions by the same procedure. The Cs^+ ions are thermally emitted from the filament.

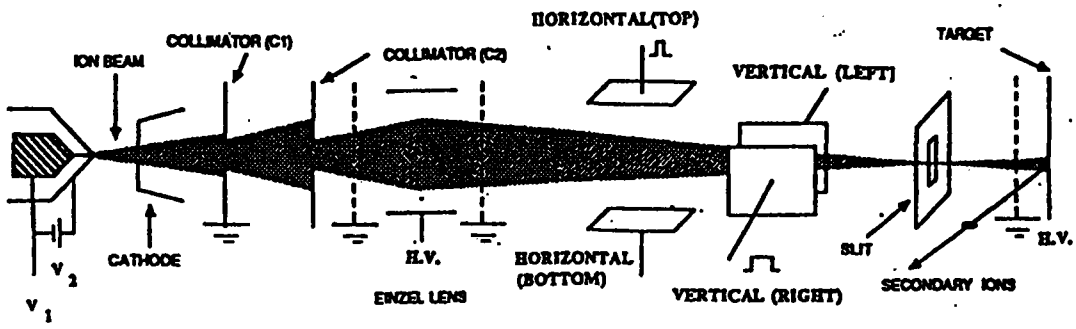

Fig. 1 Schematic diagram of the keV pulsed ion source

The filament is heated by a direct current (about 1.0 A) while it is held at a high positive potential V_1 (e.g. 30 keV) to accelerate the primary ions. The voltage of the anode shield (V_2) is a few volts higher than V_1 in order to focus the beam, and the beam is aligned with the slit by adjusting the cathode perpendicular to the beam axis. The collimator (C1) has a diameter of about 1 mm. and the other collimator (C2) can have different sizes of holes (from 5 mm to 10 mm) in a vertical line in a plane perpendicular to the ion beam axis. The ion current measured on this collimator is quite accurate and stable as it is placed very close to the filament and independent of other adjustable parameters. The ion beam is focused by a gridded einzel lens onto a vertical slit of 60 μm width. The beam is directed through the slit by applying voltages to the horizontal (BOTTOM) and vertical (LEFT) deflection plates. As required by the TOF method of mass measurements, the direct continuous beam (DC) is converted into a pulsed beam (~ 2 ns duration) by applying high voltage pulses to the vertical (RIGHT) and horizontal (TOP) plates. This technique is discussed in some detail later in this paper. The pulsed ion beam strikes the target containing thin layer of sample of organic molecules and desorbs some moleculer ions which are then accelerated and allowed to pass through a field free region of the TOF mass spectrometer. The primary ion energy can be increased up to 30 keV by varying V_1. The whole system is operated at a vacuum below 10^{-6} torr. The voltage supply to the filament and the filament shield are isolated from ground using a high voltage isolation transformer.

2.2 The pulsing mechanism

Fig. 2 shows the path of the ion beam when swept across the slit. Under DC condition (i.e. without pulsing) the beam passes through the slit. Before pulsing starts, the beam is deflected away from the slit by adjusting the DC condition. DC high voltages on the 'RIGHT' vertical and 'TOP' horizontal plates keep the beam at a point such as P just before pulsing. When pulsing is executed, the voltages on the 'RIGHT' vertical and 'TOP' horizontal plates drop from higher values to zero (e.g. from 1000 V to 0 V in case the initial energy of the primary ions is 30 keV) with a delay (e.g. 1 μs) as shown in the Fig. 3. The purpose of the

high voltage pulse applied by the vertical plate with longer pulse width is to prevent the ion beam retracing the slit during the falling edge of the pulse applied by the 'TOP' horizontal plate.

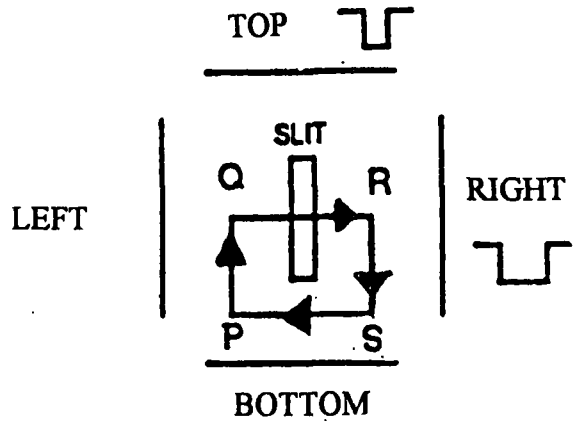

Fig. 2 The pulsing sequence of the pulser.

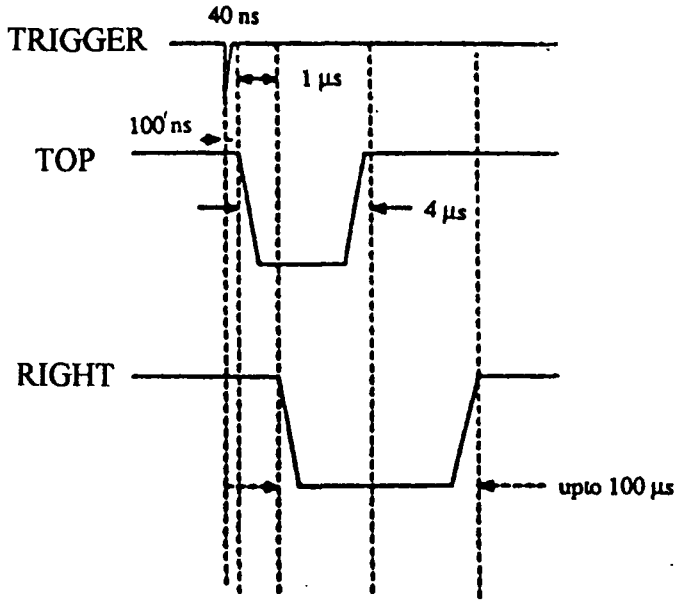

Fig. 3. Timing of the pulsing sequence.

The duration of an ion burst passing through the slit is generally dependent on the initial acceleration voltage of the ions, the mass of the ion and the value of the deflection voltage. A typical pulse length of an ion bunch is about 2 ns. By changing the filament current, the ion current on the plate of the slit can be varied from 0.1 nA to 50 nA. The pulsing frequency used is 2 kHz.

2.3 Electronics

The block diagram of the electronics associated with the ion source is shown in Fig. 4. The fast signal from the pulsing unit is used with a delay (1.5 ns) to start the time-to-digital converter (TDC) through a discriminator (DISC) for the time measurement. The quality of the spectrum can be optimised by changing the voltage on the 'LEFT' vertical plate slightly. The time resolution can be further optimised by changing the voltage on the einzel lens. The best time resolution obtained with a short flight tube (15 cm) is 1.6 ns (FWHM) for the H^+ peak in a mass spectrum of valine.

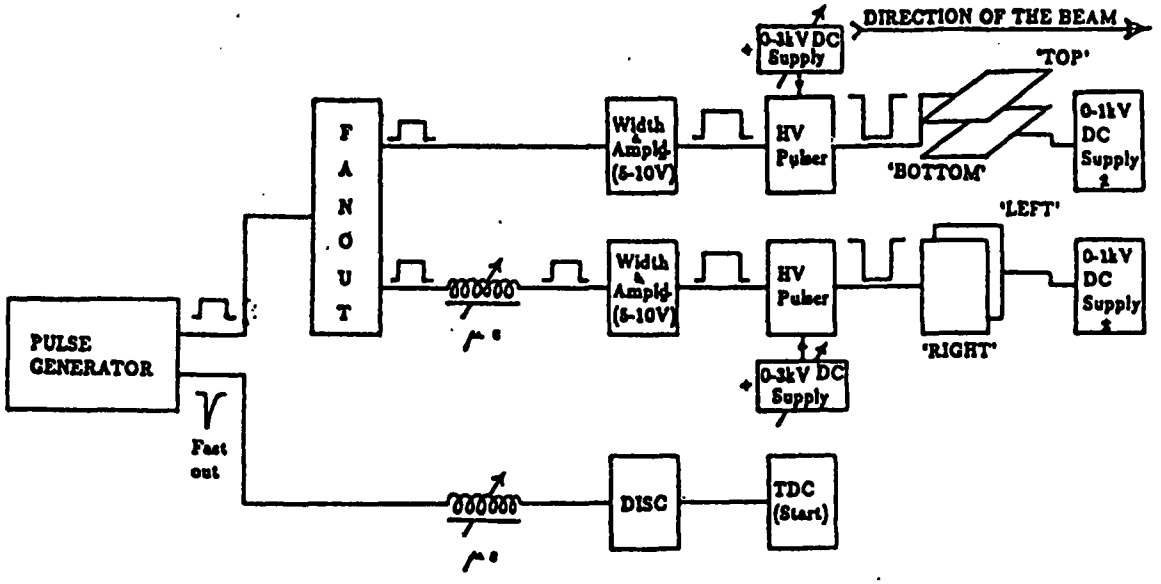

Fig. 4. Block diagram of the electronics of the keV pulsed ion source.

3. EXPERIMENTAL

3.1 Sample preparation

The valine sample was prepared by the electrospray technique[6]. The LHRH sample was prepared by adsorbing the molecules onto nitrocellulose surface[7]. The solvent used for valine was a mixture of tri fluoro acetic acid (TFA) and acetic acid (1:5 mixture) and the solvent used for LHRH was 0.1 % aqueous TFA and ethyl alcohol (1:1).

3.2 The time-of-flight mass spectrometer

The Cs^+ ions from the ion source strikes the thin organic layer of the sample which is deposited on an aluminium backing. The desorbed and ionized secondary ions are then accelerated and allowed to pass through a field free region before they strike the stop detector, see Fig. 5. The stop detector consists of two microchannel plates operated in tandem. The stop signal is passed through an amplifier and a discriminator before reaching the time to digital converter (TDC). A pulse from the pulse generator is used as the start signal of the time-of-flight measurement as well as for triggering the pulsing sequence of the ion beam. The TDC converts the time measurement into a digital pulse and then passes it into an on-line computer (Atari St 1040) where the time-of-flight spectrum is recorded and analysed.

In the first stage of the work, tuning of the ion source was carried out to optimise the performance of the ion source in order to produce a good TOF spectrum, in respect of secondary ion yield, time resolution and signal to noise ratio. The optimization was done as follows. First of all, for an arbitrary filament current, the ion beam was detected on the collimator (C2) which could be used as an ion collector (i.e. a Faraday cup) when blocking the beam line. The collimator current was maximized by adjusting the focusing voltage on the filament. Once this was done, the beam was allowed to pass through the collimator and its presence at the slit (ie on the plate where the slit is cut) was detected by observing the ion current on the slit. Then the beam was allowed to pass through the slit by adjusting the voltages on the deflection plates and subsequently it was detected on the target by observing the target current. The target current was maximized by adjusting the voltages on the einzel

lens and the voltages on the deflection plates. After all these adjustments are completed, the ion beam could be pulsed and a TOF spectrum could be collected. The pulsing current at the target was typically at the femto ampere range compared to the current at nano ampere range obtained with the DC beam.

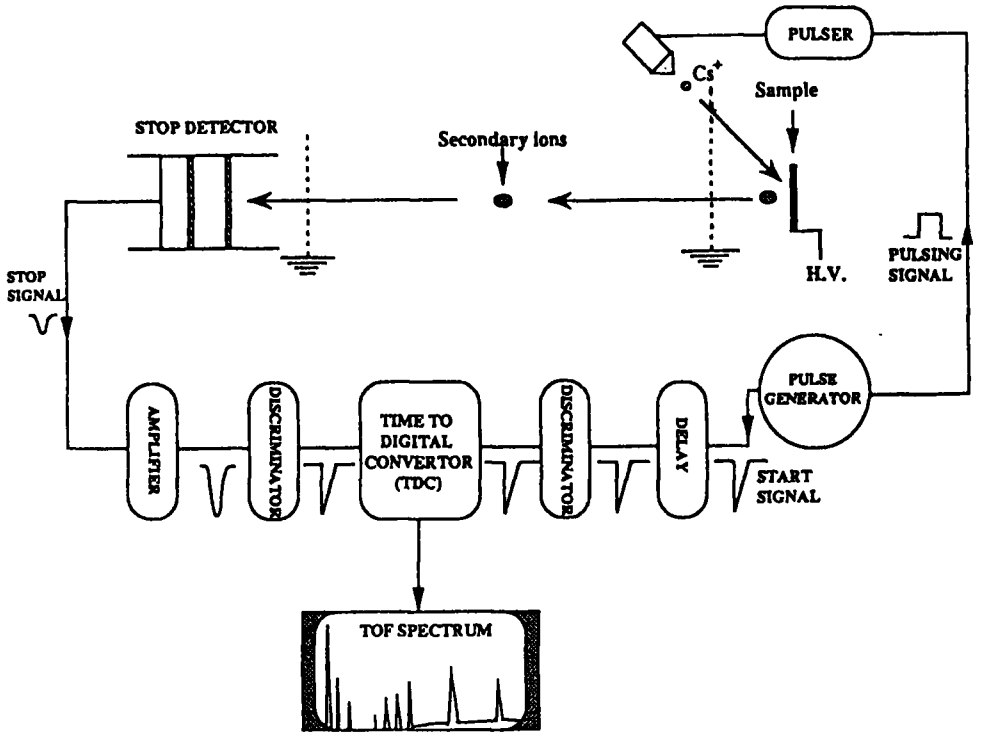

Fig. 5 Schematic diagram of the time-of-flight mass spectrometer coupled with the keV ion source

3.3 Measurement of damage cross section

A proper measurement of the ion dose (i.e. the number of Cs^+ ions per irradiation) on the sample was essential in order to obtain a precise value for damage cross section. During the course of experiments, it was realised that the direct measurement of the primary ion dose on the sample was not accurate enough due to the charging of the sample surface resulting in an errornous target current. The time integration of the target current was not an accurate measure of the number of primary ions impinged on the target either. The emission of secondary electrons from the target during irradiation also caused an extra contribution to the positive ion current on target. (An earlier used procedure was to measure the target current on the semicircular metal surface of the target holder.) This source of secondary electrons however, was suppressed by applying a small negative potential on the grid in front of the target but the charging of the target could not be avoided completely. Therefore an alternative method was devised to measure the dose indirectly by monitoring the ion current on the collimator (C2) and on the slit. This method was found to be more reliable than the earlier method as explained below.

It is possible to determine the beam current, I_t , striking the target by measuring the beam current I_S (also referred to as slit current in the text) on the plate where the slit is cut as it forms an effective Faraday cup. When the ion beam is allowed to pass through the slit, the target current is equal to the decrease, ΔI_S, in the slit current, I_S , When the beam is optimized to pass through the slit, $I_t = \Delta I_S$. It was observed experimentally that the ratio of the beam current striking the target (so determined) to the collimator current I_C,was a constant independent of the absolute current. Then using the value of this constant ratio, $\Delta I_S/I_C$, the

integrated beam current on the target (Q_t) can be calculated from the integrated current on the collimator (Q_c) using:

$$Q_t = Q_c (\Delta I_s / I_c)$$

In order to measure the damage cross section, first the molecular ion yield from a fresh target was obtained by running the TOF mass spectrometer in the analysing mode and it was followed by an irradiation damage of the target with a DC ion current.

The damaged sample area was calculated after tracing the shape of the damaged spot under a microscope. The damaged area was in the order of 10^{-3} cm^2.

4. RESULTS

4.1 Performance of the keV ion source

The mass spectra obtained with bombardment of 10 keV Cs^+ ions on a solid target consist of similar molecular ion related peaks to those in the mass spectra obtained with bombardment of MeV ^{252}Cf fission fragments on the same sample (Fig. 6 and Fig. 7) except for lower yield (i.e. the number of secondary ions desorbed per primary ion) and lower resolution values being obtained with the former. There are some dissimilarity in the spectra as far as the relative intensities and the presence of new peaks are concerned. The keV spectrum (Fig.6) has a significant peak at 132.9 u which is not found in the spectrum due to MeV ions (Fig. 7). This can be attributed to the desorption of deposited Cs^+ ions on the sample from the primary ion beam while operating the mass spectrometer in the analysing mode. The appearance of a higher intensity peak at 26.9 u (which is Al^+ peak) in the keV ion spectrum (Fig.6) compared to that in MeV ion spectrum (Fig. 7) may be due to the fact that keV ions are more efficient in desorbing metal ions than the MeV ions. The relative intensity of the fragment ion $(M-COOH)^+$ at 72 u is higher in MeV ion spectrum. This can be due to the extensive fragmentation capability of MeV ions compared to keV ions.

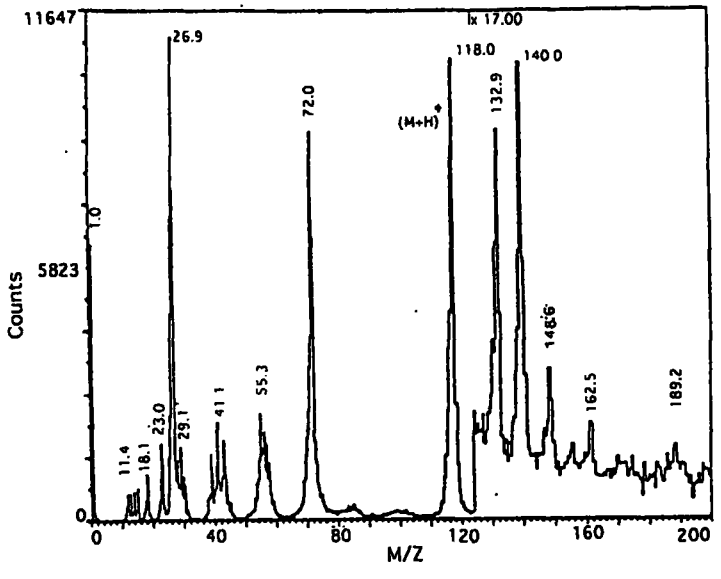

Fig. 6 Positive ion mass spectrum of valine (117 u) due to 10 keV energy (Cs^+) primary ions.

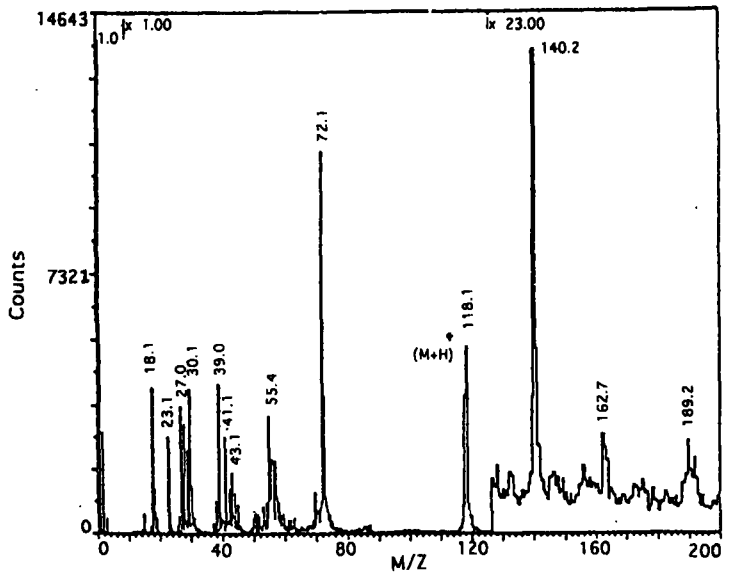

Fig. 7 Positive ion mass spectrum of valine (117 u) due to MeV energy ^{252}Cf fission fragments.

4.2 The radiation damage of biomolecules due to bombardment with Cs^+ ions in the keV range

The direct ion beam was used to irradiate the samples and after each exposure, a mass spectrum of the samples were obtained to measure the yields of the quasi molecular ion $(M+H)^+$, where M is the mass of the biomolecule. As a result of irradiation, a drastic decrease of the intensity of the parent like molecular ion, $(M+H)^+$, was observed for both compounds, valine and LHRH. Fig. 8 shows this effect for valine, and a similar trend has been observed for LHRH too. It is clearly seen from the spectra that even the intensity of all higher molecular weight ions too have gone down due to irradiation. The behavior of the normalized ion yield of $(M+H)^+$ ion as a function of ion dose at 18 keV for LHRH is shown in Fig. 9. The damage cross sections for valine and LHRH due to the bombardment of 10 keV and 18 keV Cs^+ ions are shown in Table 1.

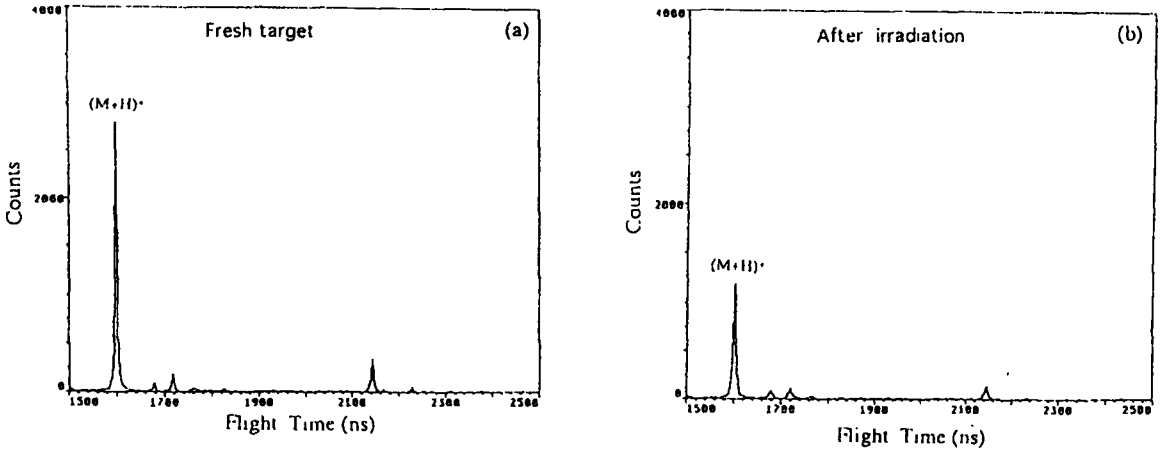

Fig. 8. The intensity of $(M+H)^+$ peak (a) from a fresh valine target and (b) from the same target after being irradiated with 4.11 x 10^{13} Cs^+ ions of 10 keV energy. Both of these time-of-flight spectra have been collected for the same duration of time with the same ion current in order to compare the intensity of the peak before and after irradiation.

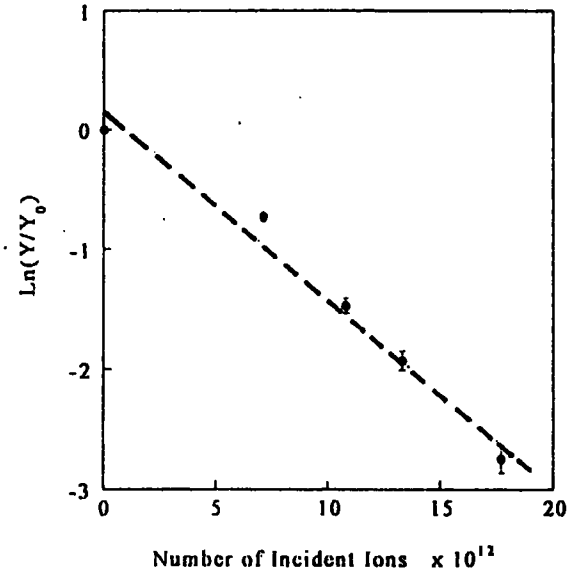

Fig. 9. The variation of the normalised ion yield of $(M+H)^+$ of LHRH as a function of number of incident Cs^+ ions used to irradiate at 18 keV energy.

Table 1. Damage cross section due to 10 keV and 18 keV Cs^+ ions

Target compound	Valine (MW=117 u).	LHRH (MW=1182 u)
Damage cross section (σ) due to 10 keV Cs^+ ions (x 10^{-14} cm^2)	2.4 ± 0.2	7 ± 1
Damage cross section (σ) due to 18 keV Cs^+ ions (x 10^{-14} cm^2)	2.5 ± 0.2	50 ± 5

5. DISCUSSION AND CONCLUSIONS

Present work has demonstrated that a pulsed low energy (keV) ion source can be constructed and coupled to an existing PDMS-TOF mass spectrometer as an alternative primary ion source to produce TOF mass spectra and to study the radiation damage cross section for biomolecules due to keV ions. The mass spectra collected using keV Cs^+ ions possess similarity as far as the presence of quasi molecular ion (e.g. $(M+H)^+$) peaks and some of the major fragment ions are concerned. The absolute secondary ion yield was found to be significantly lower and the mass resolution was found to be slightly lower for keV ions than for the MeV ions. The lower yield with keV ions may be attributed to the fact that the low energy primary ions are less efficient[9] in desorbing larger biomolecules compared to MeV energy fission fragments of ^{252}Cf. The lower resolution may arise due to the finite pulse width of the primary ion bursts impinging on the sample surface. The resolution could be improved by decreasing the slit width or increasing the pulsing frequency of the ion beam, which will reduce the pulse width of the primary ions. However, in such a case, the intensity of the ion current has to be increased to compensate for the reduction in the yield.

The damage cross sections obtained from the present study for valine are in the same order of magnitude as the damage cross sections found by Sichtermann and co-workers[2] for the amino acid leucine (MW = 131 u) ($\sigma = 6 \times 10^{-14}$ cm^2) due to keV Ar^+ ions, and one order of magnitude less than the damage cross section for valine due to MeV ions ($\sigma = 6.8 \times 10^{-13}$ cm^2) reported by Salehpour and co-workers[8]. This could be related to the fact that MeV ions are more efficient in desorbing molecules from a solid surface due to larger interaction volume in the ion track[9]. The late chemical effects may also contribute to a larger damage cross section in the case of MeV ions as discussed in the ion track model[10]. With MeV ions, Salehpour et al. have found about 7 fold increase in the damage cross section ($\sigma = 50 \times 10^{-13}$ cm^2) for a heavy biomolecule, bovine insulin (MW=5733 u), compared to valine (MW = 117 u). In the present study too, a significant increase in the damage cross section for a heavy molecule, LHRH, was observed in comparison to valine.(see Table 1). Since the LHRH molecule is larger than valine, once a small part of LHRH molecule is damaged, it will not contribute to the molecular ion peak in the time-of-flight spectrum. In addition, this enhancement in the damage cross section may be due to the fragile nature of the LHRH molecule compared to a smaller molecule such as valine.

The damage cross section for LHRH is considerably larger for 18 keV Cs^+ ions than for 10 keV Cs^+ ions (see Table 1). This could be attributed to the fact that, being a larger organic molecule, LHRH may have high probability for breaking a part of its bonds leading to fragmentation resulting in the decrease in ion yield. It has also been mentioned in the theoretical description[11] of keV sputtering that more aggressive collision mechanisms are involved with the increase in primary ion energy in the keV range. This may also contribute to some extent for the increase in damage with the increase of the ion energy.

ACKNOWLEDGEMENT

This work was supported by the Swedish Natural Science Research Council. D.D.N.B.D. and T.R.A. thank the International Program in Physical Sciences (IPPS) at the University of Uppsala, Sweden , for fellowships.

6. REFERENCES

1. Macfarlane, R. D. and Torgerson, D. F., *Science*, **191**, 920 (1976).
2. Sichtermann, W. and Benninghoven, V., *Int. J. Mass Spectrom. Ion Phys.* **40**, 177 (1981).
3. Chait, B. J. and Standing, K. G., *Int. J. Mass Spectrom. Ion Phys.* **40**, 185 (1981).
4. Blewett, J. P. and Jones, E. J., *Phys. Rev.* **50**, 464 (1936).
5. Allison, S. K. and Tamegai, M., *Rev. Sci. Instrum.* **32**, 1090 (1961).
6. McNeal, C. J., Macfarlane, R. D. and Thurston, E. L., *Anal. Chem.* **51**, 2036 (1979).
7. Jonsson, G., Hedin, A., Håkansson, P., Sundqvist, B. U. R., Säve, G., Nielsen, P., Roepstorff, P., Johansson, K. E., Kamensky, I. and Lindberg, M., *Anal. Chem.* **58**, 1084 (1986).
8. Salehpour, M., Håkansson, P. and Sundqvist, B., *Nuclear Instr. Meth B* **2**, 752-756 (1984).
9. Kamensky, I., Håkansson, P. and Sundqvist, B., *Nucl. Instr. Meth.* **198**, 65 (1982).
10. Hedin, A., Håkansson, P., Sundqvist, B. and Johnson, R. E., *Phys. Rev. B* **31**, 489 (1976).
11. Sigmund, P., *Fundamental Processes in Sputtering of Atoms and Molecules (SPUT 92), Det Kon. Dan. Vid Sel. Mat-Fhys Med.*, **43**,7 (1993)